Phase-Coded FMCW Lidar

Sebastian Banzhaf
Corporate Sector Research and Advance Engineering
Robert Bosch GmbH
Renningen, Germany
sebastian.banzhaf@de.bosch.com

Christian Waldschmidt
Institute of Microwave Engineering
Ulm University
Ulm, Germany
christian.waldschmidt@uni-ulm.de

***Abstract*—Light detection and ranging (lidar) is considered to play an important role for future advanced driver assistance systems and autonomous driving. Coherent lidar systems, which have several benefits over conventional direct detection systems, are commonly modulated by frequency modulated continuous wave (FMCW). However, FMCW lidar systems can face severe ambiguities due to high Doppler shifts or in multi-target scenarios. Hence, this paper presents a novel modulation approach for coherent lidar that combines conventional FMCW with a pseudorandom binary phase code in order to overcome possible ambiguities while maintaining a lean system setup. The proposed approach is evaluated by simulations and measurements revealing similar single-target performance as a FMCW reference system with an ideal quadrature demodulator.**

***Index Terms*—coherent lidar, FMCW, phase modulation, pseudo random binary sequences (PRBS)**

I. Introduction

The success of both advanced driver assistance systems and fully autonomous driving depends greatly on the performance of sensors that perceive the vehicular surroundings like camera, radar and lidar. In this context, lidar sensors are considered to play an important role since they are capable of acquiring precise distance estimates of targets at high angular resolutions [1], [2]. In comparison to common direct detection systems, lidar sensors with a coherent detection system offer accurate and immediate velocity estimation and hold enhanced detection performance as well as robustness against interference [1], [3]. On the other hand, coherent systems need narrow-band laser sources and suitable modulation to properly estimate both distance and velocity. Generally, lidar systems must be able to process weak receive (RX) signals whose power cannot be increased unlimitedly by higher transmit (TX) powers due to eye safety regulations. Additionally, if the lidar sensor is realized as single-pixel system, the measurement duration per pixel must be in the microsecond range to meet the frame rate specifications of automotive applications [4]. This requires on the one hand efficient signal processing algorithms and on the other hand few and short transmission sequences as well as sensor parallelization that is preferably realized by multiplexing. The single pixel architecture reduces the demand for multi-target capability even though transparent or reflective media can still cause multi-target scenarios.

A commonly used modulation approach is FMCW that transmits one up- and one down-ramp sequence per pixel. FMCW was originally proposed for radar systems but was transferred to lidar [5], [6]. In general, however, such transfers from radar to lidar are often not trivial due to lidar's shorter measurement times and significantly higher Doppler shifts. Nevertheless, FMCW enables simple baseband signal processing via fast Fourier transform (FFT) and high detection performances. Additionally, direct frequency modulation is possible by e.g. varying the gain current of the laser diode. However, if a non-quadrature demodulator is used, the lidar inherent high Doppler shift may result in an undetectable sign change of one beating frequency causing severe ambiguities in the distance and velocity estimation [7]. These ambiguities can be tackled with the help of a quadrature demodulator, which in turn requires a second receive channel leading to higher component count and cost. Additionally, phase- and gain imbalances plus the RX signal split lead to reduced performance. Furthermore, dual-sequential FMCW lidar systems have no multi-target capability and cannot readily be multiplexed without adding external components or extending the system bandwidth for each channel. An alternative to FMCW are PRBS that are applied via phase modulation to the carrier. Such phase-coded systems avoid severe ambiguities, even if a non-quadrature demodulator is used and provide multi-target capability as well as the potential for straightforward multiplexing utilizing orthogonal codes [8]. However, to achieve a comparable distance resolution to the FMCW approach, high code bandwidths are required necessitating an equally high bandwidth of the receiver.

To merge the advantages of both domains, a novel modulation method for coherent lidar that combines FMCW with a low-bandwidth phase code is presented in this paper. The new coded FMCW approach works with a simple non-quadrature demodulator and allows unambiguous distance and velocity estimation even in case of sign changes of baseband frequencies. Additionally, the approach is multi-target capable and holds the potential for multiplexing via orthogonal codes. After a theoretical introduction, starting with a short repetition of a conventional FMCW lidar system, the performance of the approach will be evaluated by simulations followed by a measurement-based feasibility validation.

II. FMCW Lidar

A. Transmission and Reception

An FMCW lidar sensor can be set up according to Fig. 1 (a) and (b) with a non-quadrature or a quadrature demodulator.

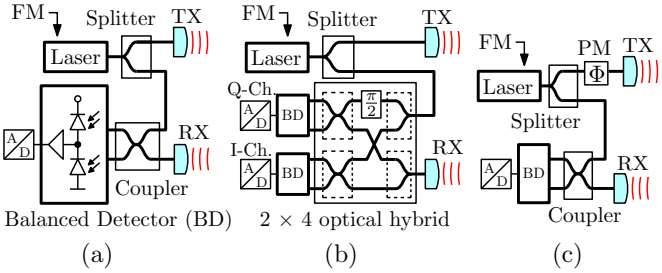

Fig. 1. Schematic illustrations of coherent FMCW lidar systems: (a) Conventional with non-quadrature demodulator, (b) conventional with quadrature demodulator and (c) coded with non-quadrature demodulator.

The frequency modulation may be implemented by direct laser modulation, which commonly utilizes a triangular pattern defined by modulation bandwidth B_{M} and sequence duration T_{M} as shown in Fig. 2 (a). The modulated signal is split into a reference signal and a TX signal. The TX signal propagates at the speed of light c_0 and hits N_{t} targets that all reflect a portion of the signal power back to the receiver. Those backscattered signals are delayed by the corresponding time of flight τ_i and shifted in frequency by the Doppler frequency $f_{\mathrm{D},i}$ (cf. Fig. 2 (a)). In the receiver, the signals are superposed additively.

B. Non-Quadrature Demodulator

For a system setup with a non-quadrature demodulator, the RX signal is combined with the reference signal by a coupler and given into a balanced detector. With the substitutions $\alpha = 2\pi(B_{\mathrm{M}}/T_{\mathrm{M}})$, $\Phi_{\mathrm{RX},i} = \omega_0\tau_i - 0.5\,\alpha\tau_i^2$ and the angular beating frequency $\omega_{\mathrm{B1},i} = \alpha\tau_i + \omega_{\mathrm{D},i}$, where ω_0 and $\omega_{\mathrm{D},i}$ denote the angular frequencies of carrier and Doppler, the time-discretized multi-target baseband signal of the up-ramp can be described by

$$s_{\mathrm{nq1}}(k) = \sum_{i=0}^{N_{\mathrm{t}}-1} A_i \cos(\Phi_{\mathrm{RX},i} + \omega_{\mathrm{B1},i} k T_{\mathrm{s}}) + n(k) \tag{1}$$

in case coupler and balanced detector are ideal. Here, A_i serves as generic signal amplitude, T_{s} is the sampling period and $k \in \mathbb{N}_0$ where $k = 0$ corresponds to the start of the up-ramp transmission. Equation (1) is valid within $\lceil \tau_{\max} f_s \rceil \leq k \leq \lceil T_{\mathrm{M}} f_s \rceil$ where $\lceil \cdot \rceil$ denotes rounding to the next greater integer and $\tau_{\max}$ describes the largest occurring time of flight. The term n is a general noise term that summarizes all noise. Analogously, the time-discretized multi-target baseband signal of the down-ramp is defined by

$$s_{\mathrm{nq2}}(k) = \sum_{i=0}^{N_{\mathrm{t}}-1} A_i \cos(\Phi'_{\mathrm{RX},i} - \omega_{\mathrm{B2},i} k T_{\mathrm{s}}) + n(k), \tag{2}$$

where $\Phi'_{\mathrm{RX},i} = (\omega_0 + B_{\mathrm{M}})\tau_i + 0.5\,\alpha\tau_i^2$ and $\omega_{\mathrm{B2},i} = \alpha\tau_i - \omega_{\mathrm{D},i}$. Equation (2) is valid within $\lceil (\tau_{\max} + T_{\mathrm{M}}) f_s \rceil \leq k \leq \lceil 2T_{\mathrm{M}} f_s \rceil$. Depending on its distance d_i and velocity v_i, each i-th target causes the beating frequencies $f_{\mathrm{B1},i}$ and $f_{\mathrm{B2},i}$, which can be determined by a frequency analysis method like the discrete Fourier transform (DFT) and subsequent peak localization. For correct determination of distance and velocity, the estimated beating frequencies $\tilde{f}_{\mathrm{B1},i}$ and $\tilde{f}_{\mathrm{B2},i}$ need to be matched correctly, which in general is not possible for multi-target scenarios, as they cannot be distinguished from other present beating frequencies. Additionally, since a non-quadrature demodulator just delivers a real baseband signal, only the absolute values of the beating frequencies are estimated leading to the two hypotheses:

(H1) $f_{\mathrm{B1},i} \geq 0$, $f_{\mathrm{B2},i} \leq 0$. Condition: $|f_{\mathrm{D},i}| \leq (B_{\mathrm{M}}/T_{\mathrm{M}})\tau_i$,
(H2) $f_{\mathrm{B1},i} \lesseqgtr 0$, $f_{\mathrm{B2},i} \lesseqgtr 0$. Condition: $|f_{\mathrm{D},i}| > (B_{\mathrm{M}}/T_{\mathrm{M}})\tau_i$,

In the single-target case and with the substitutions $\tau = 2d/c_0$ and $f_{\mathrm{D}} = 2v/\lambda_0$, where λ_0 denotes the nominal laser wavelength, the two hypotheses for distance and velocity estimate are given by

$$\tilde{d}_{\mathrm{H1,H2}} = \left| |\tilde{f}_{\mathrm{B1}}| \pm |\tilde{f}_{\mathrm{B2}}| \right| \cdot \frac{c_0 T_{\mathrm{M}}}{4B_{\mathrm{M}}}, \tag{3}$$

and

$$\tilde{v}_{\mathrm{H1,H2}} = \begin{cases} +\frac{\lambda_0}{4}(|\tilde{f}_{\mathrm{B1}}| - |\tilde{f}_{\mathrm{B2}}|) & \text{for H1} \\ +\frac{\lambda_0}{4}(|\tilde{f}_{\mathrm{B1}}| + |\tilde{f}_{\mathrm{B2}}|) & \text{for H2 and } |\tilde{f}_{\mathrm{B1}}| - |\tilde{f}_{\mathrm{B2}}| \geq 0, \\ -\frac{\lambda_0}{4}(|\tilde{f}_{\mathrm{B1}}| + |\tilde{f}_{\mathrm{B2}}|) & \text{for H2 and } |\tilde{f}_{\mathrm{B1}}| - |\tilde{f}_{\mathrm{B2}}| < 0. \end{cases} \tag{4}$$

C. Quadrature Demodulator

The algebraic sign ambiguity discussed before can be avoided using a quadrature demodulator. Here, RX and reference signal are fed into an 2×4 optical hybrid of which an exemplary structure can be seen in Fig. 1 (b). The output signals of the 2×4 optical hybrid are given into two balanced detectors whose output signals are sampled and can be combined to a complex baseband signal. In case both balanced detectors and all couplers are ideal and identical in their parameters, the time-discretized multi-target baseband signal of the up-ramp can be described by

$$s_{\mathrm{q1}}(k) = \sum_{i=0}^{N_{\mathrm{t}}-1} 0.5\, A_i e^{j\Phi_{\mathrm{RX},i}} e^{j\omega_{\mathrm{B1},i} k T_{\mathrm{s}}} + \underline{n}(k) \tag{5}$$

and the respective down-ramp baseband signal by

$$s_{\mathrm{q2}}(k) = \sum_{i=0}^{N_{\mathrm{t}}-1} 0.5\, A_i e^{j\Phi'_{\mathrm{RX},i}} e^{-j\omega_{\mathrm{B2},i} k T_{\mathrm{s}}} + \underline{n}(k). \tag{6}$$

Equations (5) and (6) are valid for the same values of k as (1) and (2). The total noise of I and Q channel is described by $\underline{n} = n_{\mathrm{I}} + j n_{\mathrm{Q}}$. The further processing is identical to the non-quadrature demodulator case. For the single-target case, the estimations are unambiguously given by $\tilde{d} = (\tilde{f}_{\mathrm{B1}} - \tilde{f}_{\mathrm{B2}})(T_{\mathrm{M}} c_0)/(4B_{\mathrm{M}})$ and $\tilde{v} = (\tilde{f}_{\mathrm{B1}} + \tilde{f}_{\mathrm{B2}})\lambda_0/4$. With the given dual-sequential modulation pattern, however, the matching issue in case of multiple targets remains.

III. Coded FMCW Lidar

A. System Setup and Baseband Signals

To avoid estimation ambiguities without the need of a costly quadrature demodulator, a phase-coded FMCW approach is proposed. The basic idea is to use the additional information

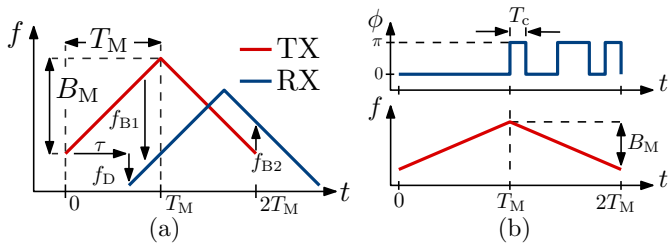

Fig. 2. (a) Triangular FMCW modulation pattern. (b) Possible modulation pattern for the coded FMCW approach

given by the transmitted code to perform plausibility checks on any estimation hypotheses. For that, a lidar system with phase modulator and non-quadrature demodulator, schematically depicted in Fig. 1 (c), is utilized. A possible modulation pattern is shown in Fig. 2 (b) where a phase-code is superposed on the down-ramp. If this modulation pattern is assumed, the time-discretized multi-target baseband signal of the first sequence can be described by (1) and the baseband signal of the second sequence by

$$s_{\mathrm{cf2}}(k)=\sum_{i=0}^{N_{\mathrm{t}}-1} A_i \cos(\Phi'_{\mathrm{RX},i}-\omega_{\mathrm{B2},i}kT_{\mathrm{s}}-\phi(kT_{\mathrm{s}}-\tau_i))+n(k), \quad (7)$$

where (7) is valid for values of k according to (2). The superposed phase-code ϕ in (7) is characterized by the code length N_ϕ, chip duration T_{c} and the code alphabet ϕ_n. The code can be described by

$$\phi(kT_{\mathrm{s}}) = \sum_{n=0}^{N_\phi-1} \phi_n \,\mathrm{rect}\left(\frac{kT_{\mathrm{s}} - T_{\mathrm{M}} - nT_{\mathrm{c}}}{T_{\mathrm{c}}}\right), \quad (8)$$

where $\mathrm{rect}(\cdot)$ is defined by

$$\mathrm{rect}\left(\frac{t}{T}\right)=\begin{cases}1 & \text{for } 0 \le t < T,\\ 0 & \text{otherwise.}\end{cases} \quad (9)$$

The proposed method requires the usage of binary phase-codes whose phase states must have a phase difference of π.

B. Ambiguous Estimation

The proposed method conducts distance and velocity estimation in two steps. The first step performs an ambiguous estimation as it is already known from a conventional FMCW lidar system with a non-quadrature demodulator, i.e. a frequency analysis via DFT and subsequent peak localization of both baseband signals is conducted. However, due to the superposed code in the down-ramp baseband signal, the frequency peaks in the corresponding spectrum will be broadened depending on the code bandwidth that is given by $B_{\mathrm{c}} = 1/T_{\mathrm{c}}$. The peak broadening results in decreased detection performance which can be moderated by a spectral moving average filter (SMAF) of even length z defined by

$$y_{\mathrm{SMAF}}(h) = \frac{1}{z}\sum_{i=-z/2}^{z/2-1} |y(h-i)|, \quad (10)$$

where y denotes the amplitude values of the frequency spectrum [8]. Without further broadening of the already broadened signal peak, the filter removes noise spikes and thus reduces the probability of false detection. In (10), $y(h-i) = 0$ for $(h-i) < 0$ and $(h-i) > N$ where $h \in \mathbb{N}$. The filter length z can be described by a ratio r of the superposed code bandwidth B_{c} given by $z = 2\lceil 0.5rNB_{\mathrm{c}}T_{\mathrm{s}}\rceil$ where N denotes the DFT length. For a single-target scenario, peak localization within up- and averaged down-ramp spectra delivers the frequency estimates $\tilde{f}_{\mathrm{B1}}$ and $\tilde{f}_{\mathrm{B2,SMAF}}$ whose signs are unknown due to the non-quadrature demodulation. Hence, in accordance to section II-B, there are two hypothetical estimation pairs for distance and velocity: d_{H1}, v_{H1} and d_{H2}, v_{H2}.

C. Plausibility Check

The second step of the proposed method performs plausibility checks using the superposed code to resolve any ambiguousness caused by non-quadrature demodulation or multiple targets. For this, the coded baseband signal is multiplied with the known code sequence, which is shifted based on the existing hypotheses. This *code unfolding* procedure, introduced in [8], provides the signal

$$u(k,x) = s_{\mathrm{cf2}}(k) \cdot \cos(\phi((k-x)T_{\mathrm{s}})). \quad (11)$$

Given a biphase code satisfying $\phi_n = \{0, \pi\}$, (11) can be transformed into

$$u(k,x)=\sum_{i=0}^{N_{\mathrm{t}}-1} A_i \cos(\Phi'_{\mathrm{RX},i}-\omega_{\mathrm{B2},i}kT_{\mathrm{s}}-\phi(kT_{\mathrm{s}}-\tau_i)+\phi((k-x)T_{\mathrm{s}})) + n(k)\cos(\phi((k-x)T_{\mathrm{s}})), \quad (12)$$

by inserting (7). If $x = x_i = \tau_i/T_{\mathrm{s}}$, the code will be removed for the i-th target, so that only the angular beating frequency $\omega_{\mathrm{B2},i}$ remains in the argument of the corresponding cosine function. For any other condition of x, a residual code remains in the signal. Therefore, a correct hypothesis can be detected by frequency analysis and peak quality evaluation of $u(k, x_{\mathrm{H}})$ where $x_{\mathrm{H}} = 2d_{\mathrm{H}}/(c_0T_{\mathrm{s}})$ and d_{H} denotes a preestimated hypothetical distance. That way, all hypotheses from the first step can be evaluated. By performing another peak localization within the unfolded frequency spectrum of the hypothesis considered correct, the existing distance and velocity estimates can be updated in a more precise manner.

IV. Results

In this section, the performance and feasibility of the proposed method will be evaluated by simulations and measurements. Initially, the most relevant modulation parameters are discussed.

A. Parameter Discussion

1) Duration and System Bandwidth: Both ramps of the frequency modulation and the superposed phase code have a duration of T_{M} resulting in a total measurement time per pixel of $2T_{\mathrm{M}}$. Generally, a longer sequence duration increases the measurement performance due to the processing gain of the

TABLE I
PARAMETERS OF SIMULATED LIDAR SYSTEM

Parameter	Symbol	Value	Parameter	Symbol	Value
Max. distance	$d_{\max}$	180 m	Code type	–	MLS
Max. abs. velocity	$\lvert v_{\max}\rvert$	80 ms^{-1}	Number of targets	N_{t}	1
Carrier wavelength	λ_0	1550 nm	DFT length	N	4096
FMCW bandwidth	B_{M}	500 MHz	SMAF filter ratio	r	2/3
Sequence duration	T_{M}	10 μs			

DFT but does also decrease the measurement rate of the lidar sensor. The bandwidth of the system can be approximated by $B_{\mathrm{sys}} \approx (2B_{\mathrm{M}}d_{\max})/(T_{\mathrm{M}}c_0) + f_{\mathrm{D,max}} + B_c$, where, however, B_{c} is typically negligibly small.

2) Resolution and Accuracy: In comparison to conventional FMCW, the superposed phase code implies reduced resolution and estimation accuracy of the first processing step since one beating frequency peak is broadened. Utilizing Gaussian error propagation, distance and velocity resolution after the first processing step of the coded FMCW method can be approximated by $\Delta d_\phi = c_0(1 + B_{\mathrm{c}}T_{\mathrm{M}})/(4B_{\mathrm{M}})$ and $\Delta v_\phi = \lambda_0(1+B_{\mathrm{c}}T_{\mathrm{M}})/(4T_{\mathrm{M}})$. If the code is perfectly removed from the signal during the subsequent unfolding procedure, the updated estimates will have the same resolution as for standard FMCW, i.e. $\Delta d = c_0/(2B_{\mathrm{M}})$ and $\Delta v = \lambda_0/(2T_{\mathrm{M}})$.

3) Code Bandwidth: The code bandwidth B_{c} influences both processing steps of the coded FMCW method. A fast, high-bandwidth code results in a broader and flatter spectral representation of the coded beating frequency within the first processing step. This leads to a reduced detection performance, which can be partially moderated by spectral averaging. On the other hand, the higher the bandwidth of the code, the more precise the shift of the code template must correspond to the true distance to get a good unfolding result in the second step. Hence, the hypotheses evaluation becomes more robust.

B. Simulation

In this section, the proposed coded FMCW method will be evaluated by simulation. A lidar system according to Fig. 1 (c), with the modulation pattern from Fig. 2 (b) and the parameters from Table I is considered; the used code is based on a maximum length sequence (MLS). To allow comparison with an FMCW reference system, only a single-target is simulated. For deciding which hypothesis is correct, a constant false alarm rate (CFAR) threshold is calculated for both frequency spectra that are obtained after unfolding the coded baseband signal with both distance hypotheses. Subsequently, the maximum peak to threshold values are compared and the spectrum with the higher value is considered to represent the correct hypothesis.

1) Analysis of Plausibility Check: In the following, the performance of the hypotheses decision will be analyzed by simulations that employ different target velocities and one constant target distance. That way, the beating frequencies will take all possible values including values close to zero. Those lead to a more difficult determination of which hypothesis

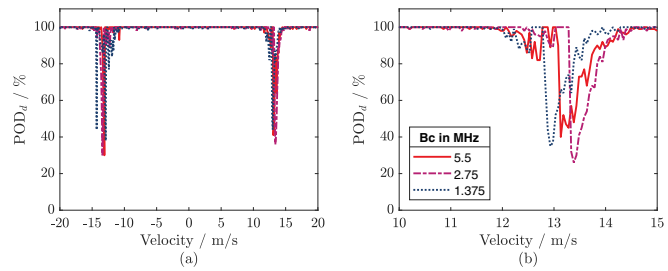

Fig. 3. Simulated distance POD over target velocity at constant target distance $d = 50$ m for different superposed code bandwidths B_{c}. Each velocity value is simulated 100 times. (a) Full range with 0.1 m/s velocity spacing and (b) region of interest with 0.05 m/s velocity spacing.

is correct since the estimation and unfolding results of both hypotheses become more similar (cf. (3) to (4)). Fig. 3 shows the simulated probability of detection (POD) values for the distance estimation of a coded FMCW lidar system at a target distance of 50 m for velocities in the range ± 20 m/s and various superposed code bandwidths. Since distance and velocity estimation show the same behavior, only the graph for the distance estimation is shown. A detection is considered correct if the corresponding estimate satisfies $|\tilde{d} - d| \leq 2\Delta d$ or respectively $|\tilde{v} - v| \leq 2\Delta v$ where Δd and Δv correspond to the FMCW resolution given in IV-A2. The velocity value for which one of the beating frequencies becomes zero, can be calculated by $v_{\mathrm{fz}} = \pm(B_{\mathrm{M}}\lambda_0 d)/(T_{\mathrm{M}}c_0)$. For the given scenario, v_{fz} is approx. ± 12.92 m/s. Fig. 3 (a) illustrates that for all used codes the POD drops significantly around v_{fz}; Fig. 3 (b) shows that independently from the superposed code bandwidth, the results are quite similar even if position and width of the POD drop vary in some degree. Here, the width tends to be slightly larger for slow codes.

2) Probability of Detection and Accuracy: In this section, the overall POD performance and accuracy of the coded FMCW approach is simulated for several target distances and compared to an FMCW reference system with a quadrature demodulator. The accuracy is described by the root mean square error (RMSE) of all successful detections. The condition for a successful detection corresponds to the one from section IV-B1. The graphs in Fig. 4 show the POD and RMSE values for ground truth distances in the range between 30 m to 180 m in 5 m steps. For each distance step, velocity values from an interval of ± 80 m/s at a spacing of 0.4 m/s are simulated 10 times. Fig. 4 (a) and (b) demonstrate that the POD performance of the coded FMCW approach is only slightly worse than that of the FMCW reference system (cf. IQ-Reference curve). This performance loss can be interpreted as the price paid for the benefits of the proposed method. Within the simulated code bandwidths, higher bandwidths lead to worse results. However, code bandwidths further below the simulated ones will also lead to a gradual performance degradation. The RMSE values of the coded FMCW approach in Fig. 4 (c) and (d) are just about identical to the reference.

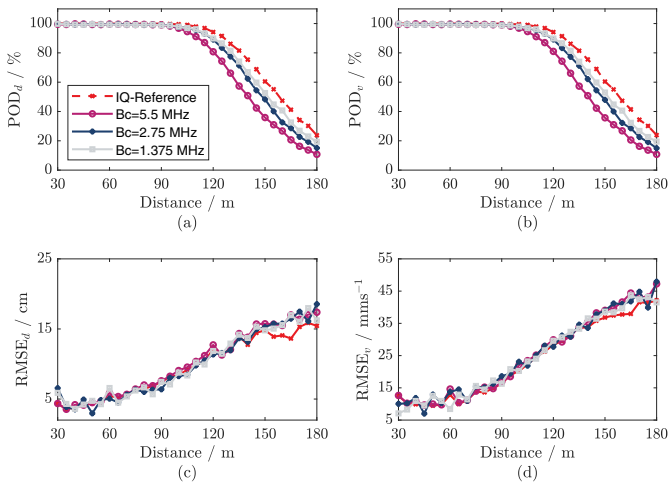

Fig. 4. Simulated performance indicators for different superposed code bandwidths over target distance: (a) Distance POD, (b) velocity POD, (c) distance RMSE and (d) velocity RMSE.

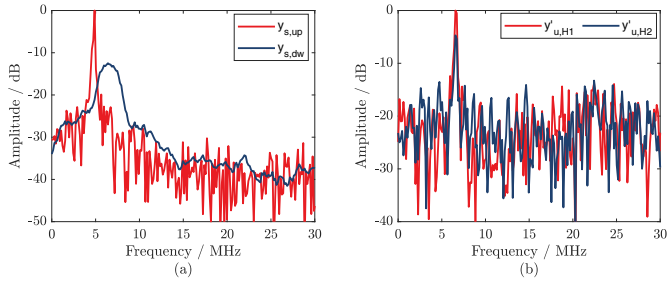

Fig. 5. Measurement results for the scenario $d_1 = 4.7\,\mathrm{m}$, $v_1 = -0.65\,\mathrm{m/s}$. (a) Frequency spectra of beating signals where the down ramp spectra was spectrally averaged, (b) relative frequency spectra for both hypotheses after unfolding. $N_{\mathrm{DFT}} = 8196$, $B_{\mathrm{c}} = 2\,\mathrm{MHz}$.

C. Measurement

To verify that the proposed coded FMCW approach is feasible, measurements in a laboratory environment have been conducted. The setup of the used fiber-based demonstrator corresponds to the schematic illustration from Fig. 1 (c) supplemented by an additional delay line in the TX path of 15 m. As target served a rotatable tilted disc covered with retro-reflector foil, whose rotation speed sets target velocity. Unless not otherwise stated, the measurement parameters correspond to the simulation parameters from Table I. Fig. 5 (a) shows the frequency spectra of the beating signals where a spectral moving average filter has been applied to the coded down ramp signal. Fig. 5 (b) on the other hand shows the relative frequency spectra y' of the unfolded signals that represent the ratio between frequency spectrum and CFAR threshold. Even though the beating frequencies are only in the lower MHz range meaning that both hypotheses are rather similar, the relative spectra curves in Fig. 5 (b) clearly show an amplitude about 4.7 dB higher for the first hypothesis indicating its correctness.

TABLE II
COMPARISON BETWEEN CONVENTIONAL AND THE CODED FMCW

Criteria	FMCW		Coded FMCW
Demodulator	Quadrature	Non-quadrature	
d-v Ambiguity	No	Yes	No
Multi-target capability	No	No	Yes
Multiplexing potential	Low	Low	High
Performance	4.5 / 5	5 / 5	4 / 5
Computational complexity	2×complex FFT	2×real FFT	4×real FFT

D. Comparison

Table II compares the conventional FMCW approaches with the proposed coded FMCW approach. The performance is ranked qualitatively; neglecting potential ambiguities, using a scale from 1 to 5, where 5 indicates excellent performance. Additionally, the computational complexity is assessed by the number of required FFT calculations per measurement.

V. CONCLUSION

In this paper, a novel modulation approach for coherent lidar that combines triangular FMCW with a pseudorandom binary phase code has been presented. The approach overcomes disadvantages of conventional FMCW lidar systems allowing for unambiguous estimation, multi-target capability and straightforward multiplexing via orthogonal codes. In contrast to an FMCW system with quadrature demodulator, the proposed method provides also a lean system setup enabling a less complex design and reduced component cost. The simulation analysis has shown that the performance of the method, in terms of probability of detection and accuracy, is comparable to a conventional FMCW lidar system with quadrature demodulator.

REFERENCES

[1] Y. Li and J. Ibanez-Guzman, "Lidar for autonomous driving: The principles, challenges, and trends for automotive lidar and perception systems," *IEEE Signal Processing Magazine*, vol. 37, no. 4, pp. 50–61, 2020.
[2] R. H. Rasshofer and K. Gresser, "Automotive radar and lidar systems for next generation driver assistance functions," *Advances in Radio Science*, vol. 3, pp. 205–209, 2005.
[3] P. McManamon, "Review of ladar: a historic, yet emerging, sensor technology with rich phenomenology," *Optical Engineering*, vol. 51, no. 6, pp. 1 – 14, 2012.
[4] M. E. Warren, "Automotive lidar technology," in *2019 Symposium on VLSI Circuits*, 2019, pp. C254–C255.
[5] F. Roos, J. Bechter, C. Knill, B. Schweizer, and C. Waldschmidt, "Radar sensors for autonomous driving: Modulation schemes and interference mitigation," *IEEE Microw. Mag.*, vol. 20, no. 9, pp. 58–72, 2019.
[6] D. Pierrottet, F. Amzajerdian, L. Petway, B. Barnes, G. Lockard, and M. Rubio, "Linear FMCW laser radar for precision range and vector velocity measurements," *MRS Proceedings*, vol. 1076, pp. 1076–K04–06, 2008.
[7] Z. Xu, H. Zhang, K. Chen, D. Zhu, and S. Pan, "FMCW lidar using phase-diversity coherent detection to avoid signal aliasing," *IEEE Photon. Technol. Lett.*, vol. 31, no. 22, pp. 1822–1825, 2019.
[8] S. Banzhaf and C. Waldschmidt, "Phase-Code-Based Modulation for Coherent Lidar," submitted for publication at IEEE Transactions on Vehicular Technology.